IOP Conf. Series: Journal of Physics: Conf. Series **783** (2017) 012015 doi:10.1088/1742-6596/783/1/012015

A Hybrid Extended Kalman Filter as an Observer for a Pot-Electro-Magnetic Actuator

Simon Schmidt, Paolo Mercorelli

Institute of Product and Process Innovation, Leuphana University of Lueneburg, Volgershall 1, D-21339 Lueneburg, Germany

E-mail: {simon.schmidt, mercorelli}@uni.leuphana.de

Abstract. This paper deals with an application in which a *hybrid* extended Kalman Filter (HEKF) is used to estimate state variables in a U-shaped electro-magnetic actuator to be used in mechanical systems. In this context a hybrid Kalman Filter is the one which switches between different models. The paper proposes a hybrid model for an extended Kalman Filter to be used as an observer to estimate the state and to control the force of the actuator. Applications include position, velocity and force control in automotive, engine and manufacturing systems. This work is focused on the estimation of state variables of the actuator. Simulated results show the effectiveness of the proposed approach.

1. Introduction

Dynamic systems are usually classified as continuous or discrete dynamic ones. However, real systems cannot often be clearly classified into one of these categories. Most real dynamic systems contain continuous and discrete dynamics as well. This mixture of continuous and discrete dynamics is called a hybrid dynamic system (or short: hybrid system). Therefore, hybrid dynamic systems exhibit continuous and instantaneous changes, having features of continuous-time and discrete-time dynamical systems. Many examples of hybrid systems are given not only from physics, but also from automotive and industrial applications. Hybrid systems can be not only found in modern technologies in which continuous variables are mixed with non-continuous ones. An overview on this literature can be found in [1] and in [2]. Very often just the necessity of reconfigurations of the controller as well as the observer generate many difficulties as shown in [3]. Nevertheless, in electro-magnetic mechanical actuators, observers as in [4], [5] and in particular Kalman Filter (KF) as an observer such as in [6] and [7] are very often applied. In [8] an electromagnetic mechanical actuator for engines is considered. In this application the kernel of the actuator is represented by a U-shaped electromagnetic actuator, which controls the intake and exhaust valve for engines. In contrast to this work, the contribution of this paper is oriented to the control of an actuator to be used in manufacturing systems for the problem of precise positioning. In applications it is often desirable to implement control without a position sensor due to the restricted mounting space and the expense. In this case, an estimator could be the basis for sensorless control in which position and velocity signals are reconstructed from electrical measurements [9, 10]. Another challenging problem, for reasons of safety is represented by the soft landing of the positioning. Achieving a soft landing is a difficult job that requires precise state estimation. To achieve sensorless control, in the literature, there are several different

approaches propose which are based on observers. The Kalman Filter is one of the most used algorithms in this context, with the extended version utilized when nonlinearities are present in the system. The extended Kalman Filter (EKF) is a heuristic method for nonlinear filtering and estimation problems. When it is tuned well, it is often effective and is widely used in practice. Nevertheless, the EKF needs to be enhanced and adapted to the particular application; in this case, the EKF is a viable and computationally efficient candidate for general applications. In general, applications of Kalman Filters offer the possibility of implementing a state-based controller in any field with automatic controls. An adaptive extended Kalman Filter has been used to improve the performance of industrial drive control by estimating some important loads of the industrial drive [11]. A novel sensorless force control approach for robot-assisted motion of the human arm based on the Kalman Filter has been presented in [12] as well as an intelligent system that incorporates Kalman Filters and a fuzzy expert system to track the tip of a fastening tool and to identify the fastened bolt [13]. In general, because these control structures avoid bulky and complicated measurement systems, they are easily applicable to real world problems. The proposed method presented in this paper is general and can be applied to all types of problems in which position and velocity measurements are not possible or are too expensive to be acquired.

2. Contribution of the paper

The proposed method presented in this paper is quite general and could be applied to all types of problems in which position and velocity measurements are not possible or are too expensive to be acquired. The main contributions of this paper are as follows:

- the introduction of an observer for a sensorless control scheme
- the use of a hybrid extended Kalman Filter based on five switching models

This paper provides an extensive description of an application combining a hysteresis hybrid observer with an extended Kalman Filter and hysteresis automation, resulting in sensorless control. The hybrid observer scheme is designed to expand upon the continuous extended Kalman Filter. The proposed structure consists of five models. Between these models there are five switching conditions to make sure that the observer works inside the correct region of the state space. An artificial hysteresis between the switching states is introduced to avoid chattering problems when the velocity is close to zero. The proposal considers already consolidated structures on extended Kalman Filter and uses theory of hybrid systems to get a hybrid structure of this filter. Using this combination of well known approaches yields to a new structure of Kalman Filter, which shows a very accurate and fast observation of states. The proposed observer works in the way that the current is measured, and the position and velocity of the electromagnet are estimated. The behavior of the system is a hybrid one, because it has points in state space where it switches its behavior. These switching points are met e.g. on upper or lower limits. The paper is organized as follows. In Section 4, a hybrid model of the actuator is presented. In Section 3 fundamental aspects of KF are recalled together with the description of the structure of the proposed EKF which is devoted to estimate the state variables of the actuator. In particular Section 5 presents the validations of the proposed approach though simulations and also shows the performance of the proposed observer. Conclusion closes the paper.

3. Tracking embedded hybrid behaviors using an Extended Kalman Filter

Our state estimation architecture tracks the nominal system dynamics using a robust observer scheme implemented as a combination of an Extended Kalman Filter (EKF) and an automated switching between several models for the magnet. The hybrid observer has to track (i) continuous behavior in individual modes of operation and (ii) discrete mode changes. At mode changes,

the new state space model and the initial state of the system are recomputed, and the error covariance matrix is updated. The hybrid observer scheme is designed to expand upon the continuous extended Kalman Filter. Hysteresis is introduced to avoid chattering problems when the velocity is close to zero. Model uncertainty and measurement noise are implemented as white noise, using uncorrelated Gaussian distributions with zero mean. To be able to estimate the operation mode, the model discussed in section 4 is extended by an additional state and then it is as follows:

$$\dot{\mathbf{x}} = \mathbf{f}_q(\mathbf{x}(t)) + \mathbf{g}(t)u(t) + \mathbf{w}(t), \tag{1}$$

$$\mathbf{x}(t) = \begin{bmatrix} i(t) \\ s(t) \\ v(t) \\ q(t) \end{bmatrix}, \quad \mathbf{g}(t) = \begin{bmatrix} \frac{1}{L(s(t))} \\ 0 \\ 0 \\ 0 \end{bmatrix}, \tag{2}$$

where function $\mathbf{f}$ represents the nonlinearities, and $\mathbf{w}(t)$ is the model uncertainty. The measured output can be written as follows:

$$y(t) = \mathbf{H}_m\mathbf{x}(t) + \zeta(t), \tag{3}$$

where $\mathbf{H}_m = [1 \;\; 0 \;\; 0 \;\; 0]$, and $\zeta(t)$ is the measurement noise variance. An EKF is based on linearized dynamics, output functions at the current estimate and on propagating an approximation of the conditional expectation and covariance. In the prediction mode q, the predicted state is

$$\mathbf{x}(k/k-1) = \mathbf{x}(k-1/k-1) + T_s\big(\mathbf{f}_q(\mathbf{x}(k-1/k-1)) + \mathbf{B}_m\mathbf{u}(k-1)\big), \tag{4}$$

and the predicted error covariance matrix is

$$\begin{aligned}\mathbf{P}_q(k/k-1) = \mathbf{P}_q(k-1/k-1) + T_s\big(&\mathbf{F}_q(x(k-1/k-1))\mathbf{P}_q(k-1/k-1) \\ &+ \mathbf{P}_q(k-1/k-1)\mathbf{F}_q(x(k-1/k-1))\big) + \mathbf{R}_w,\end{aligned} \tag{5}$$

where $k \in \mathbb{Z}$, $\mathbf{R}_w$ is the process noise covariance matrix, $\mathbf{P}_q(k-1/k-1)$ is the error covariance matrix, $\mathbf{F}_q(x(k-1/k-1))$ is the Jacobian matrix of the system calculated at the estimated state, and T_s is the sampling time.
In particular, the Jacobian matrix $\mathbf{F}_q(\mathbf{x}(k-1/k-1))$ and $\mathbf{P}_q(k-1/k-1)$ with variable $q \in \mathbb{N}$, where $q = 1, 2, ..., 5$ are related to the five dynamic modes of the actuator. In the correction mode,

$$\mathbf{K}_q(k) = \mathbf{P}_q(k/k-1)\mathbf{H}_m^T\big(\mathbf{H}_m\mathbf{P}(k/k-1)\mathbf{H}_m^T + \mathbf{R}_\zeta\big)^{-1} \tag{6}$$

$$\mathbf{x}(k/k) = \mathbf{x}(k/k-1) + \mathbf{K}_q(k)\big(y(k) - \mathbf{H}_m\mathbf{x}(k/k-1)\big) \tag{7}$$

$$\mathbf{P}_q(k/k) = \mathbf{P}_q(k/k-1) - \mathbf{K}_q(k)\mathbf{H}_m\mathbf{P}_q(k/k-1), \tag{8}$$

where $\mathbf{K}_q(k)$ is the Kalman gain and $\mathbf{R}_\zeta$ is the measurement noise matrix. The mode change calculations are based on the system mode at time step k, $q(k)$, and on the state of the system $\mathbf{x}(k)$. In contrast to the standard extended Kalman Filter there are discontinuities because of the switching state $q(t)$. To make sure that the observer works in a robust way, all states has to be recalculated at switching points and the Kalman Filter has to use different models for the differnt modes of operation.

4. Description of the actuator and its hybrid mathematical model

Figures 1 and 2 represent a simplified scheme of the U-shaped Electromagnetic actuator which is proposed to be observed. The general mathematical model can be found in the literature such as [14]. To test the proposed algorithm, an actuator is considered. The actuator consists only of

Figure 1. Simplified scheme of pot-magnet

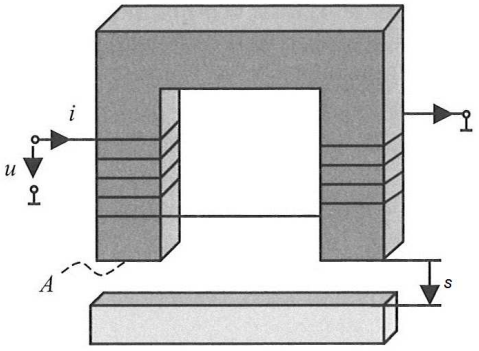

Figure 2. Free-body diagram of magnet anchor

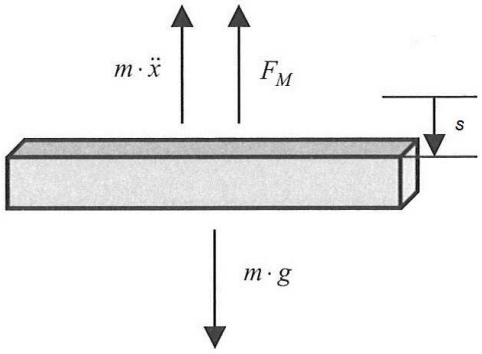

a half magnet system. The data for the physical dimensions and characteristics are taken from a real magnet. A state vector $\mathbf{x}(\mathbf{t}) = [i(t), s(t), v(t)]$ and an input voltage $u(t)$ are considered for the system in Fig. 1. The current is represented by $i(t)$, the position of the armature by $s(t)$, the velocity by $v(t)$ and the input voltage by $u(t)$. The general system can be represented in the following way. The electrical dynamics are governed by the equation

$$\frac{di(t)}{dt} = \frac{1}{L(s(t))}\Big(u(t) - \Big(R + \frac{dL(s(t))}{dt}\Big)i(t)\Big), \tag{9}$$

where $i(t)$ indicates the current, u indicates the supply voltage, R indicates the resistance and L indicates the inductance. The inductance L is a function of the current $i(t)$, through the magnetic permeability, and of the distance $s(t)$. In particular,

$$L(s(t)) = \frac{N^2 \mu_r \mu_o A}{c_1 + 2\mu_r s(t)}, \tag{10}$$

where N represents the number of windings, μ_r and μ_0 represent the relative permeability and the vacuum permeability respectively, A is the surface involved in the magnetic flux and c_1 is a physical constant that depends on the current position of the magnet. From (10) the following expression can be derived:

$$\frac{dL(s(t))}{ds} = -\frac{2N^2 \mu_r^2 \mu_o A}{(c_1 + 2\mu_r s(t))^2}. \tag{11}$$

Since there is no equation for $\frac{dL(s(t))}{dt}$ but one for $\frac{dL(s(t))}{ds}$ the following equation is needed:

$$\frac{dL(s(t))}{dt} = \frac{dL(s(t))}{ds}\frac{ds(t)}{dt} = \frac{dL(s(t))}{ds}\frac{ds(t)}{dt} = \frac{dL(s(t))}{ds}v(t). \tag{12}$$

The mechanical dynamic equation is the following:

$$\frac{d^2 s(t)}{dt^2} = \frac{F_m(t) - F_g(t)}{m}, \tag{13}$$

where $F_m(t)$ represents the magnetic force and is:

$$F_m(t) = \frac{N^2 \mu_r^2 \mu_o A i^2(t)}{(c_1 + 2\mu_r s(t))^2}, \tag{14}$$

F_g is the gravitational force. According to the range of the velocity $v(t)$ in which the actuator works, it can be considered a linear affine function of the velocity. This model can be summarized as follows:

$$\underbrace{\begin{bmatrix} \frac{di(t)}{dt} \\ \frac{ds(t)}{dt} \\ \frac{dv(t)}{dt} \end{bmatrix}}_{\dot{\mathbf{x}}(t)} = \underbrace{\begin{bmatrix} \frac{-(Ri(t)+\frac{dL(s(t))}{ds}v(t)i(t))}{L(s(t))} \\ v(t) \\ \frac{F_m(t)-F_g(t)}{m} \end{bmatrix}}_{\mathbf{f}(t)} + \underbrace{\begin{bmatrix} \frac{1}{L(s(t))} \\ 0 \\ 0 \end{bmatrix}}_{\mathbf{g}(t)} u(t). \tag{15}$$

The model described above now can be used as basis to build a more accurate model as described in the upcoming part. According to the description of the dynamic modes proposed in [14] it is possible to individuate five operation modes with five switching variables for the proposed actuator in the context of the application presented above. The state diagram represented in Fig. 3 shows the principle of the switching strategy. If variable $q \in \mathbb{N}$, where $q = 0, 1, 2, 3, 4$ are related to the five dynamic modes of the actuator, then the five phases can be described as follows:

- i. $q = 0$, Latent phase lower limit (as long as $i(t) < i_{on}$): initial conditions $\rightarrow i(0) = 0$; $s(0) = 0$; $v(0) = 0$.
- ii. $q = 1$, Lifting phase (as long as $0 < s(t) < s_{max}0$, $v(t) > 0$): initial conditions $i(0) = i_{on}$; $s(0) = 0$; $v(0) = 0$.
- iii. $q = 2$, Contact phase (as long as $s(t) = s_{max}$ and $\frac{di(t)}{dt} = 0$): initial conditions $i(0) = i(t)$; $s(t) = s_{max}$; $v(t) = 0$.
- iv. $q = 3$, Latent phase upper limit (as long as $i(t) > i_{off}$): initial conditions $\rightarrow i(0) = i(t)$; $s(0) = s_{max}$; $v(0) = 0$.
- v. $q = 4$, Back phase (as long as $v(t) < 0$ and $s(t) > 0$): initial conditions $i(0) = i_{off}$; $s(t) = s_{max}$; $v(t) = 0$.

i_{on}, i_{off} are two constant currents, s_{max} is the position in which the actuator establishes the contact. Moreover, it is possible to introduce another switching variable to identify s_{max} in which the contact phase starts and the time in which the back phase starts. To get a clear representation the following constants are used:

$$\begin{array}{llll} K_1 = \frac{N^2 \mu_r \mu_0 A}{l_1}, & K_2 = l_1, & K_3 = 2\mu_r, & K_4 = N^2 \mu_r^2 \mu_0 A \\ K_5 = N^2 \mu_r \mu_0 A, & K_6 = R_i + R_m, & K_7 = R_d + R_m. & \end{array}$$

The resistance R is changing at the position limits. At the lower limit $s(t) = 0$ the resistance is $R = K_6$. At the upper limit it is $R = K_7$.
$q = 0$: Latent phase lower limit (as long as $i(t) < i_{on}$): initial condition $\rightarrow i(0) = 0$; $s(0) = 0$; $v(0) = 0$. In this phase the inductance $L(s(t))$ is constant because the position is constant $s = 0$. Because of this, the derivative of the inductance gets zero and the system can be simplified to:

$$\underbrace{\begin{bmatrix} \frac{di(t)}{dt} \\ \frac{ds(t)}{dt} \\ \frac{dv(t)}{dt} \end{bmatrix}}_{\dot{\mathbf{x}}(t)} = \underbrace{\begin{bmatrix} \frac{-(K_6 i(t))}{K_1} \\ 0 \\ 0 \end{bmatrix}}_{\mathbf{f}(t)} + \underbrace{\begin{bmatrix} \frac{1}{K_1} \\ 0 \\ 0 \end{bmatrix}}_{\mathbf{g}(t)} u(t), \tag{16}$$

Figure 3. State diagram

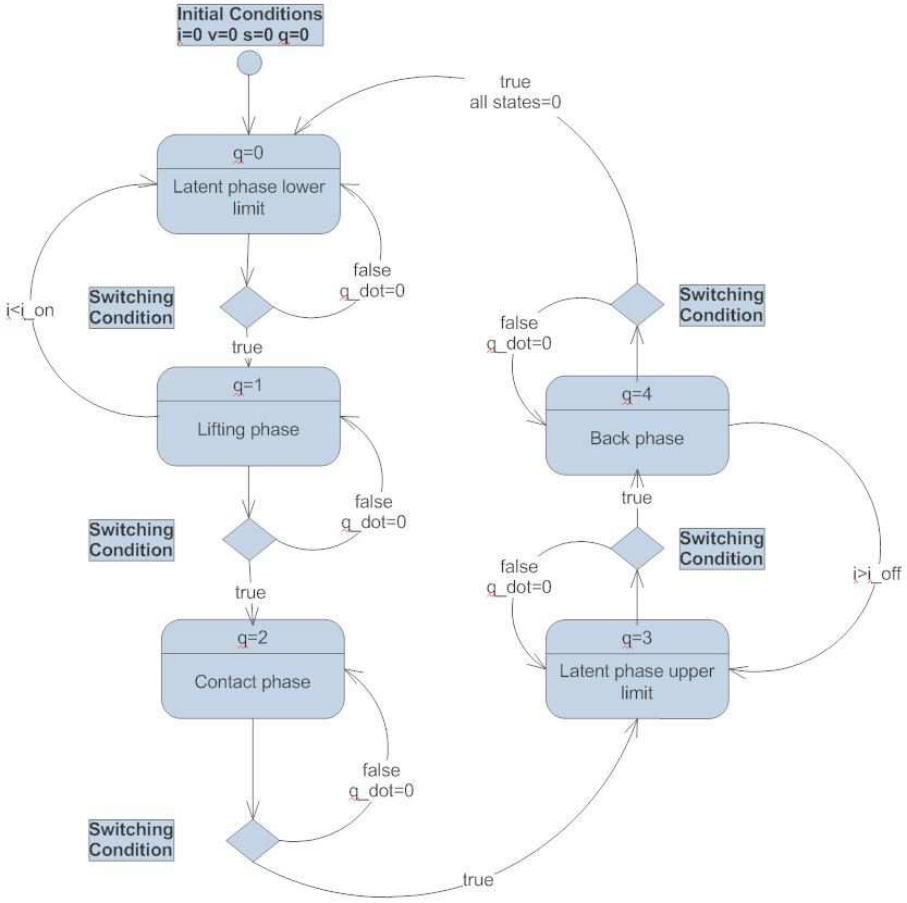

with $L(s(t)) = K_1$.
$q = 1$*: Lifting phase starting with* $i(0) = i_{on}$ *(as long as* $0 < s(t) < s_{max}$*,* $v(t) > 0$*): initial conditions* $i(0) = i_{on}$*;* $s(0) = 0$*;* $v(0) = 0$.

$$\underbrace{\begin{bmatrix} \frac{di(t)}{dt} \\ \frac{ds(t)}{dt} \\ \frac{dv(t)}{dt} \end{bmatrix}}_{\dot{\mathbf{x}}(t)} = \underbrace{\begin{bmatrix} \frac{-(K_6 i(t) + \frac{dL(s(t))}{ds} v(t) i(t))}{L(s(t))} \\ v(t) \\ \frac{F_m(t) - F_g(t)}{m} \end{bmatrix}}_{\mathbf{f}(t)} + \underbrace{\begin{bmatrix} \frac{1}{L(s(t))} \\ 0 \\ 0 \end{bmatrix}}_{\mathbf{g}(t)} u(t), \tag{17}$$

with $L(s(t)) = \frac{K_5}{(K_2 + K_3 s(t))}$, $\frac{dL(s(t))}{ds} = \frac{-2K_4}{(K_2 + K_3 s(t))^2}$ and $F_m = \frac{K_4 i(t)^2}{(K_2 + K_3 s(t))^2}$.
$q = 2$*: Contact phase (as long as* $s(t) = s_{max}$ *and* $\frac{di(t)}{dt} = 0$*): initial conditions* $i(0) = i(t)$*;*

$s(t) = s_{max}$; $v(t) = 0$.

$$\underbrace{\begin{bmatrix} \frac{di(t)}{dt} \\ \frac{ds(t)}{dt} \\ \frac{dv(t)}{dt} \end{bmatrix}}_{\dot{\mathbf{x}}(t)} = \underbrace{\begin{bmatrix} \frac{-(K_6 i(t)}{L(s(t))} \\ 0 \\ 0 \end{bmatrix}}_{\mathbf{f}(t)} + \underbrace{\begin{bmatrix} \frac{1}{L(s(t))} \\ 0 \\ 0 \end{bmatrix}}_{\mathbf{g}(t)} u(t), \tag{18}$$

with $L(s(t)) = \frac{K_5}{(K_2 + K_3 s(t))}$.
$q = 3$: *Latent phase upper limit (as long as $i(t) > i_{off}$): initial conditions $i(0) = i(t)$; $s(0) = s_{max}$; $v(0) = 0$.*

$$\underbrace{\begin{bmatrix} \frac{di(t)}{dt} \\ \frac{ds(t)}{dt} \\ \frac{dv(t)}{dt} \end{bmatrix}}_{\dot{\mathbf{x}}(t)} = \underbrace{\begin{bmatrix} \frac{-(K_7 i(t)}{K8} \\ 0 \\ 0 \end{bmatrix}}_{\mathbf{f}(t)} + \underbrace{\begin{bmatrix} \frac{1}{K_8} \\ 0 \\ 0 \end{bmatrix}}_{\mathbf{g}(t)} u(t). \tag{19}$$

$q = 4$: *Back Phase starting for $i(t) < i_{off}$ (as long as $v(t) < 0$ and $s(t) > 0$): initial condition $i(0) = i_{off}$; $s(t) = s_{max}$; $v(t) = 0$.*

$$\underbrace{\begin{bmatrix} \frac{di(t)}{dt} \\ \frac{ds(t)}{dt} \\ \frac{dv(t)}{dt} \end{bmatrix}}_{\dot{\mathbf{x}}(t)} = \underbrace{\begin{bmatrix} \frac{-(K_7 i(t) + \frac{dL(s(t))}{ds} v(t) i(t))}{L(s(t))} \\ v(t) \\ \frac{F_m(t) - F_g(t)}{m} \end{bmatrix}}_{\mathbf{f}(t)} + \underbrace{\begin{bmatrix} \frac{1}{L(s(t))} \\ 0 \\ 0 \end{bmatrix}}_{\mathbf{g}(t)} u(t), \tag{20}$$

with $L(s(t)) = \frac{K_5}{(K_2 + K_3 s(t))}$, $\frac{dL(s(t))}{ds} = \frac{-2K_4}{(K_2 + K_3 s(t))^2}$ and $F_m = \frac{K_4 i(t)^2}{(K_2 + K_3 s(t))^2}$. All these equations describe the whole hybrid system of a magnet.

5. Validation through simulations

The simulation is done with Matlab/Simulink using the 'Hybrid Equations Toolbox' developed by [15]. The constants used for the simulation are shown in Table 1. To show how the hybrid Kalman Filter is estimating the state, a simulation of the system discussed in Section 4 runs using the Hybrid Equations Toolbox. In parallel, the hybrid Extended Kalman Filter uses the current (plus added white noise) of this simulation as measurement to estimate the position $s(t)$ and the velocity $v(t)$. To show the efficiency and accuracy of this estimation several steps excite the simulation. The simulated state (black line) and estimated state (dashed/dotted red line) states are always shown in the same diagram to give a good possibility of comparison. If the magnet is already lifted and the excitation gets zero, it shows the following behavior. Now the excitation is inverted to a step from 24V to 0V at 0.5 seconds. Now the current shows the behavior as shown in Fig.4. The estimation here is nearly exact and without any delay. This is because the current is the measured state with just a small uncertainty. In Fig.6 the velocity for this kind of step is represented. The velocity is negative for a short time and then zero is reached again because the magnet reaches the lower limit. Finally Fig. 7 shows the switching variable for a step for 0V to 24V. Here the passed operation modes beginning at 0.5 seconds are 2 (Contact Phase), 3 (Latent phase upper limit) and 4 (Back Phase). Afterwards, the system gets back to operation mode 1 and is 'waiting' for an excitation. Concerning the setup parameters of the Kalman Filter, the process noise covariance matrix $\mathbf{R}_w$, the measurement noise variance

Table 1. Constants used for simulation

Constant	Description	Value
g	gravity constant	$9.81\frac{m}{s^2}$
N	number of windings	964
μ_0	vacuum permeability	$1.257e^{-3}\frac{Vs}{Am}$
μ_r	relative permeability	200
A	surface involved in the magnetic flux	$7.6341e^{-5}m^2$
s_{max}	maximum position	$0.5e^{-3}m$
m	mass of magnet armature	$0.34kg$
i_{on}	turn-on current	$0.1A$
i_{off}	cut-off current	$0.02A$
$R = R_i + R_m$	resistance on lower level	114.3Ω
$R = R_d + R_m$	resistance on upper level	120Ω
l_1	average field line length	$22e^{-6}m$
T_s	sample time	$1e^{-4}s$

Figure 4. Current for a step from 24V to 0V at 0.5 seconds

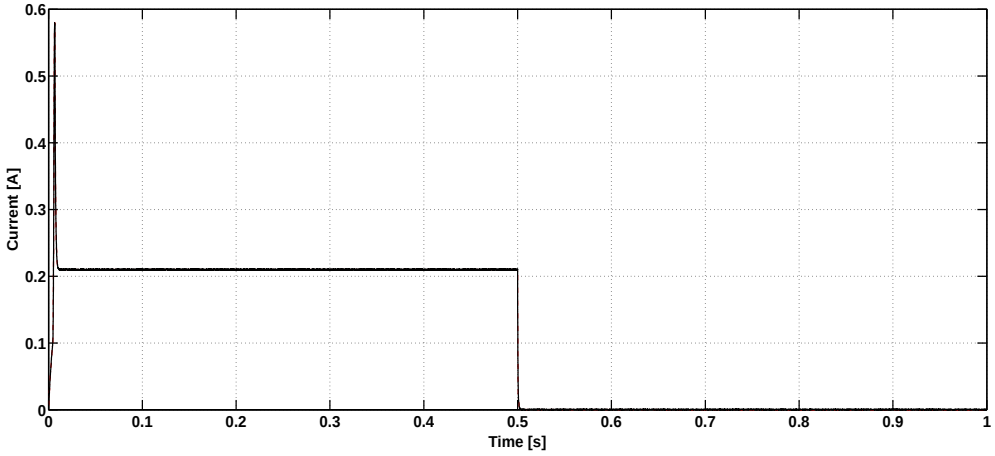

$\mathbf{R}_\zeta$ is and the initial values of the covariance matrix $\mathbf{P}_q(\mathbf{0})$ are chosen equal for each q-model and their values are as follows:

$$\mathbf{R}_w = \begin{bmatrix} 1 & 0 & 0 & 0 \\ 0 & 10^{-10} & 0 & 0 \\ 0 & 0 & 10^{-10} & 0 \\ 0 & 0 & 0 & 10^{-10} \end{bmatrix}, \tag{21}$$

$\mathbf{R}_\zeta = 0.01$ and $\mathbf{P}_q(\mathbf{0}) = \mathbf{0}$. It is possible to observe that matrix $\mathbf{R}_w$ states the precision which which the model is known. In particular, the uncertainty is localised in the first equation in which the nonlinearity is present.

Figure 5. Position for a step from 24V to 0V at 0.5 seconds

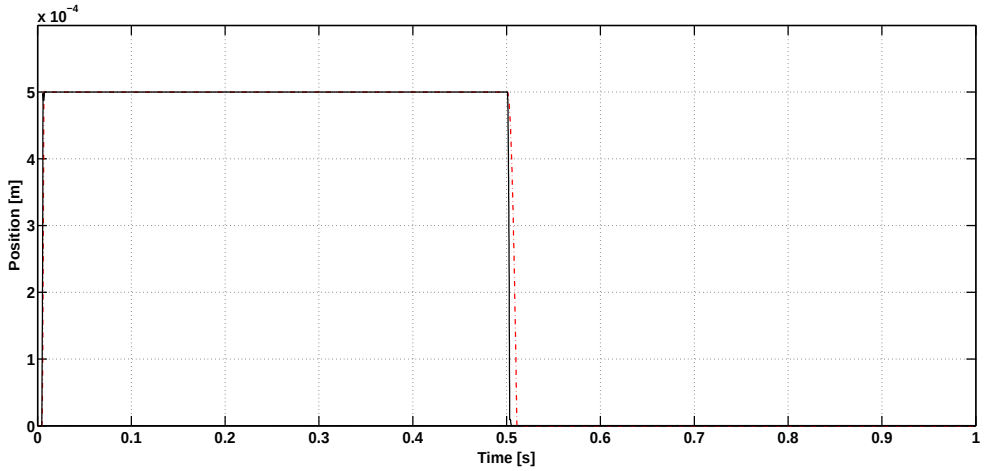

Figure 6. Velocity for a step from 24V to 0V at 0.5 seconds

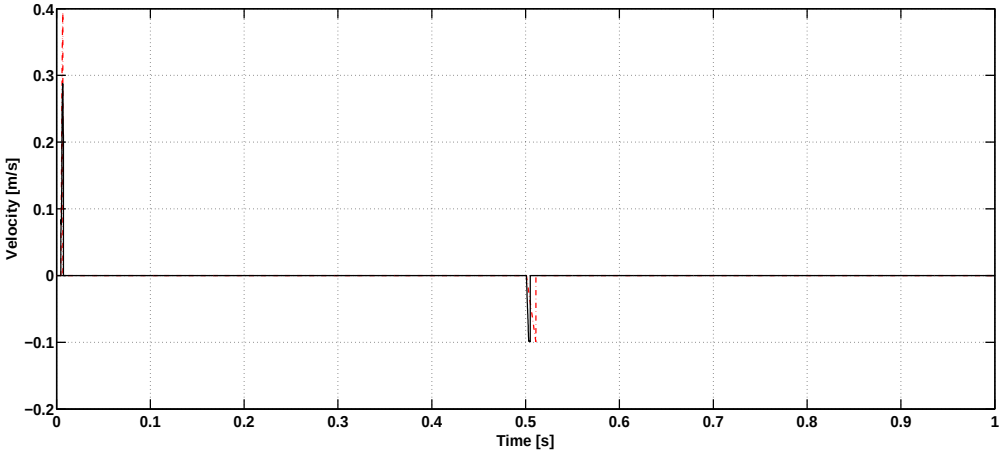

6. Performance of the proposed Observer

A performance evaluation concerning the estimation is provided using a Root-Mean-Square (RMS) Deviation (RMSD). The following RMSD of an estimator $\hat{\theta}$ with respect to an estimated parameter θ is defined as the square root of the mean square error. In case of an unbiased estimator, the square root of the mean square error corresponds to the square root of the variance, known as the standard deviation.

$$RMSD = \sqrt{MSE(\hat{\theta})} = \sqrt{E(\hat{\theta} - \theta)} \tag{22}$$

In a Kalman Filter the presence of a bias is shown to be caused by a correlation between the gain and innovation sequences which are due to the nonlinearity on the measurements, [16]. Using a linearisation, this correlation remains and to obtain an unbiased filter, a modification of the EKF is considered in [17]. The variation proposed in [17] uses a modification of the nonlinear measurement function and is claimed to give unbiased estimates. In our case, the proposed EKF does not consist of a nonlinear output function. In this case indicator RMSD is appropriately applied. In fact, the RMS Deviation (RMSD) or Root-Mean-Square Error (RMSE) is very often

Figure 7. Switching variable q for a step from 24V to 0V at 0.5 seconds

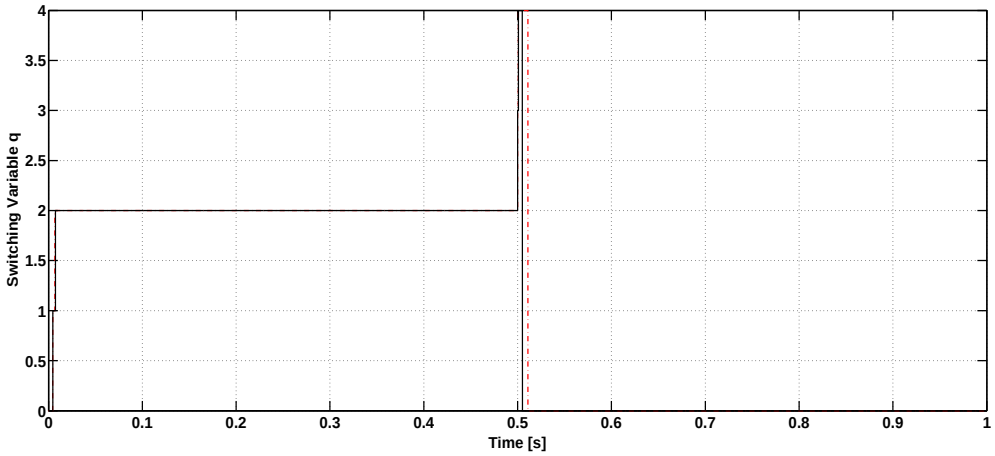

used, in particular in unbiased cases, as a measure of the differences between values predicted by a model or an estimator and the values actually observed. The RMSD represents the sample standard deviation of the differences between predicted values and observed values. These individual differences are called residuals when the calculations are performed over the data sample that was used for estimation, and are called prediction errors when computed out-of-sample. The RMSD serves to aggregate the magnitudes of the errors in predictions for various times into a single measure of predictive power. RMSD is a good measure of accuracy, but only to compare forecasting errors of different models for a particular variable and not between variables, as it is scale-dependent.

Figure 8. RMS Deviation of the Current for a step from 24V to 0V at 0.5 seconds

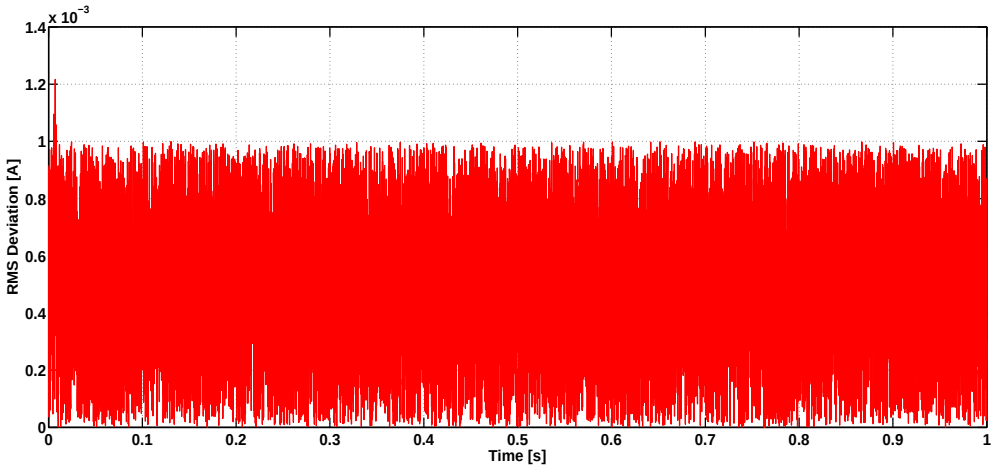

7. Conclusion

The paper deals with an application in which a hybrid extended Kalman Filter is used to estimate state variables in a Pot-Magnet to be used in mechanical systems. The paper proposes a hybrid model to be used in the extended Kalman Filter to monitor the state and to control the

Figure 9. RMS Deviation of the Position for a step from 24V to 0V at 0.5 seconds

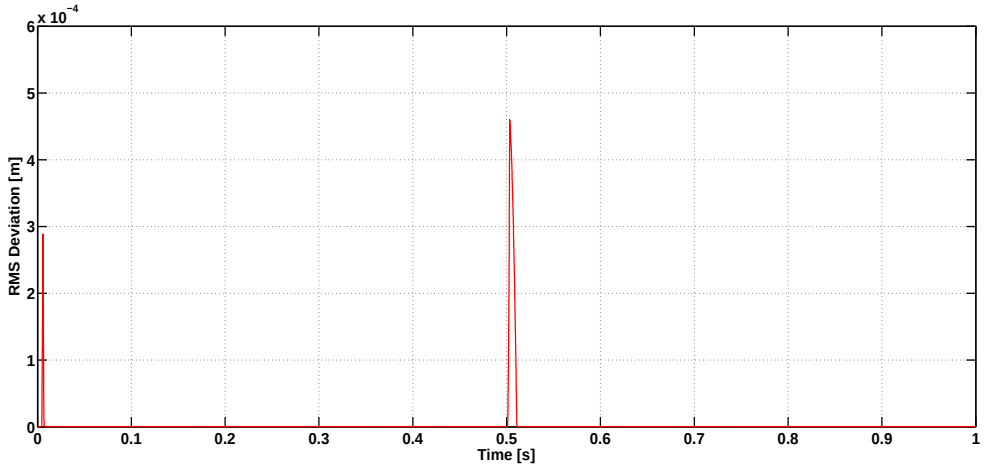

Figure 10. RMS Deviation of the Velocity for a step from 24V to 0V at 0.5 seconds

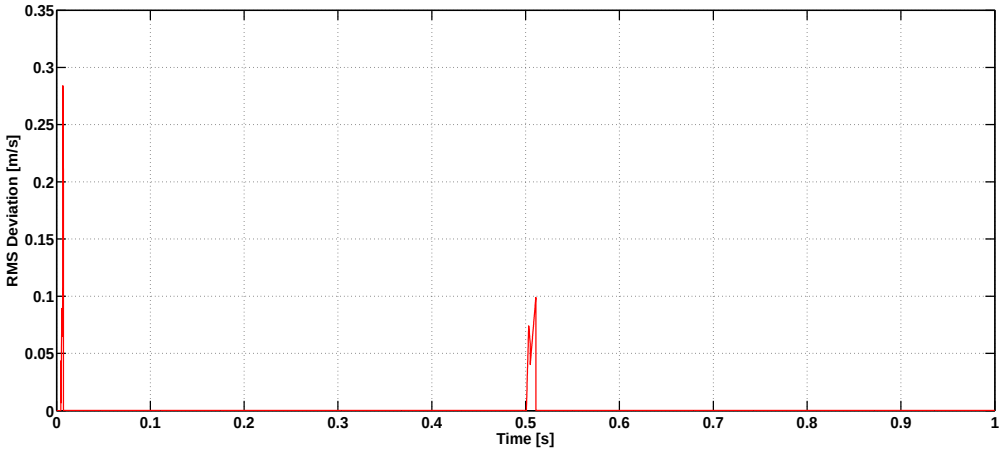

force of the actuator to be applied in manufacturing systems. Validations using simulations are shown and discussed to demonstrate the validity of the approach which proposed five dynamic models to be integrated and coordinated with a switching logic structure. The proposed observer shows a good performance and estimates the states correctly. A possible future work consists of an implementation into a real system and in designing a controller for this system using the proposed hybrid Kalman Filter.

References

[1] Goebel R., Sanfelice R.G. and Teel A 2009 Hybrid dynamical systems, *IEEE Control Systems Magazine*, **29**(2), 28–93.
[2] Sanfelice R.G. 2013 Control of Hybrid Dynamical Systems: An Overview of Recent Advances, *Control of Hybrid Dynamical Systems: An Overview of Recent Advances*, (Wiley).
[3] Mercorelli P. 2012 A Hysteresis Hybrid Extended Kalman Filter as an Observer for Sensorless Valve Control in Camless Internal Combustion Engines, *IEEE Transactions on Industry Applications*, **48**(6), 1940–1949.
[4] Mercorelli P. 2014 An Adaptive and Optimized Switching Observer for Sensorless Control of an Electromagnetic Valve Actuator in Camless Internal Combustion Engines, Robust Adaptive Soft Landing

Figure 11. RMS Deviation of the Switching variable q for a step from 24V to 0V at 0.5 seconds

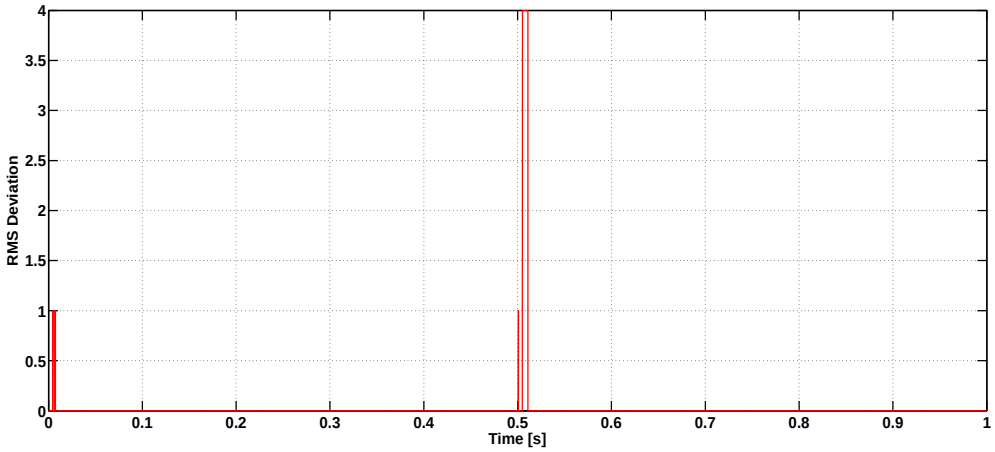

Control of an Electromagnetic Valve Actuator for Camless Engines, *Asian Journal of Control*, **16**(4), 959–973.

[5] Mercorelli P. 2016 Robust Adaptive Soft Landing Control of an Electromagnetic Valve Actuator for Camless Engines, *Asian Journal of Control*, **18**(5), 1299–1312.

[6] Mercorelli P. 2015 A Two-Stage Sliding-Mode High-Gain Observer to Reduce Uncertainties and Disturbances Effects for Sensorless Control in Automotive Applications, *IEEE Transactions on Industrial Electronics* **62**(9), 5929–5940.

[7] Mercorelli P. 2012 A Two-Stage Augmented Extended Kalman Filter as an Observer for Sensorless Valve Control in Camless Internal Combustion Engines, *IEEE Transactions on Industrial Electronics* **59**(11), 4236–4247.

[8] Mercorelli P. 2012 An Anti-Saturating Adaptive Pre-action and a Slide Surface to Achieve Soft Landing Control for Electromagnetic Actuators, *IEEE/ASME Transactions on Mechatronics*, **17**(1), 76–85.

[9] Butzmann S., Melbert J. and Koch A 2000 Sensorless control of electromagnetic actuators for variable valve train, *Proc. SAE Technical Paper 2000-01-1225*.

[10] Tai C. and Tsao T. 2003 Control of an electromechanical actuator for camless engines, *Proceedings of the American control conference* vol 4, 3113–3118.

[11] Szabat K. and Orlowska-Kowalska T. 2008 Performance Improvement of Industrial Drives With Mechanical Elasticity Using Nonlinear Adaptive Kalman Filter, *IEEE Transactions on Industrial Electronics*, **55**(3), 1075–1084.

[12] Mitsantisuk C., Katsura S. and Ohishi K. 2009 Kalman-Filter-Based Sensor Integration of Variable Power Assist Control Based on Human Stiffness Estimation, *IEEE Transactions on Industrial Electronics*, **56**(10), 3897–3905

[13] Won S., Golnaraghi F. and Melek W. 2009 A Fastening Tool Tracking System Using an IMU and a Position Sensor with Kalman Filters and a Fuzzy Expert System, *IEEE Transactions on Industrial Electronics*, **56**(5), 1782–1792.

[14] Kallenbach E., Eick R., Quendt P., Ströhla T, Feindt K, Kallenbach M and Radler O 2012 *Das dynamische Verhalten von Elektromagneten* (Wiesbaden, Germany: Vieweg+Teubner Verlag (Springer)) ISBN 9783834882974-9783834809681.

[15] Sanfelice R.G., Copp D.A. and Nanez P 2014 Hybrid equations (hyeq) toolbox v2.02 URL `https://hybrid.soe.ucsc.edu/software`

[16] Moorman M.J. and Bullock T.E. 1991 Mathematical analysis of bias in the extended kalman filter, *Proceedings of the 30th IEEE Conference on Decision and Control, 1991*, 2733–2737.

[17] Song T. and Speyer J. 1985 A stochastic analysis of a modified gain extended Kalman filter with applications to estimation with bearings only measurements, *IEEE Transactions on Automatic Control*, **30**(10), 940–949, ISSN 0018-9286.